Bone 122 (2019) 22–30

Contents lists available at ScienceDirect

Bone

journal homepage: www.elsevier.com/locate/bone

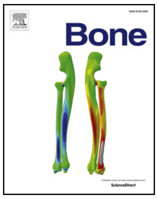

Full Length Article

Advanced glycation end-product 2 and *Porphyromonas gingivalis* lipopolysaccharide increase sclerostin expression in mouse osteocyte-like cells

Eijiro Sakamoto, Jun-ichi Kido[*], Ryosuke Takagi, Yuji Inagaki, Koji Naruishi, Toshihiko Nagata, Hiromichi Yumoto

Department of Periodontology and Endodontology, Institute of Biomedical Sciences, Tokushima University Graduate School, Tokushima, Japan

ARTICLE INFO

Keywords:
Sclerostin
Osteocyte
Diabetes mellitus
Periodontitis
AGEs
P-LPS

ABSTRACT

Sclerostin is a secreted glycoprotein that is mainly expressed in osteocytes, exerts negative effects on bone formation, and is present at elevated levels in diabetes mellitus (DM). Periodontitis is an infectious disease caused by periodontopathic bacteria, a complication of DM, and sometimes associated with severe inflammation and alveolar bone resorption. Advanced glycation end-products (AGEs) are a major pathogen in DM complications and adversely influence periodontitis in DM patients. In the present study, the effects of AGE2 and *Porphyromonas gingivalis* lipopolysaccharide (*P*-LPS) on the expression of sclerostin in mouse osteocyte-like cells (MLO-Y4-A2 cells) and its function in osteoblast differentiation were investigated. AGE2 and *P*-LPS up-regulated the expressions of receptor of AGE (RAGE) and Toll-like receptor 2 (TLR2), respectively, and significantly up-regulated that of sclerostin and interleukin 6 (IL-6) in osteocytes. Sclerostin, RAGE and TLR2 levels were synergistically increased by AGE2 and *P*-LPS. The siRNAs of RAGE and TLR2 significantly inhibited AGE2- and *P*-LPS-induced sclerostin expression. AGE2 up-regulated sclerostin expression in osteocyte-like cells via the RAGE, ERK and JNK, and NF-κB signal pathways. On the other hand, *P*-LPS elevated sclerostin levels via the TLR2, JNK and p38, and NF-κB signal pathways. When osteocytes pre-treated with AGE2 and *P*-LPS and osteoblastic cells (MC3T3-E1) were co-cultured in the medium with a sclerostin-neutralizing antibody, AGE2- and *P*-LPS-induced decreases in alkaline phosphatase activity and Runx2 expression in osteoblastic cells were significantly inhibited by the sclerostin-neutralizing antibody. These results suggest that AGE2 and *P*-LPS influence bone metabolism and inflammation through the regulation of sclerostin expression, and may aggravate periodontitis with DM.

1. Introduction

Osteocytes are the main cellular component of bone tissue [1] and play an important role in bone metabolism through the expression of several bone-related factors including receptor-activator of nuclear factor κB ligand (RANKL), dickkopf-related protein 1 (DKK1) and sclerostin [2]. Sclerostin is encoded by the SOST gene, mainly expressed in osteocytes, and detected in marrow stromal cells, osteoclast precursors and osteoblasts [3]. Sclerostin reduces osteoblastic bone formation by inhibiting the Wnt/β-catenin signaling pathway [4], and has been shown to stimulate RANKL secretion from osteocytes and induce osteoclastogenesis [5]. Bone mineral density, bone volume, osteoblast activity, and bone strength were previously reported to be reduced in transgenic mice overexpressing sclerostin [6]. Furthermore, a clinical study showed that monoclonal humanized antibodies to sclerostin significantly reduced the risk of new bone fracture and increased bone mineral density in postmenopausal women with osteoporosis [7]. Thus, sclerostin modulates bone metabolism for bone formation and resorption by inhibiting osteoblastic functions and regulating osteoclast differentiation through the modulation of RANKL levels. Circulating levels of sclerostin are elevated in diabetes mellitus (DM), menopause, osteolytic cancers, and immobilization [8]. Serum sclerostin levels were previously reported to be higher in type 1 and 2 DM patients than in non-DM individuals [9,10], and sclerostin levels have been shown to reflect bone fragility, with elevations being associated with more bone fractures in DM patients [11]. These findings suggest that sclerostin induces catabolic effects on bone metabolism in DM and its associated complications.

Periodontal diseases are chronic inflammatory diseases that are caused by multifactorial factors and mainly by Gram-negative bacteria

---

[*] Corresponding author at: 3-18-15 Kuramoto, Tokushima 770-8504, Japan.
E-mail address: kido.jun-ichi@tokushima-u.ac.jp (J.-i. Kido).

https://doi.org/10.1016/j.bone.2019.02.001
Received 3 September 2018; Received in revised form 23 January 2019; Accepted 4 February 2019

[12]. Periodontopathic bacteria, including *Porphyromonas gingivalis* (*P. gingivalis*), *Tannellera forsythia* and *Treponema denticola*, induce inflammation in periodontal tissues and degrade periodontal ligaments and alveolar bone, which ultimately results in tooth loss [13,14]. The lipopolysaccharide of *P. gingivalis* (*P*-LPS) is a potential pathogenic factor in periodontitis and leads to destructive inflammation in periodontal tissues [15]. *P*-LPS inhibits osteoblastic differentiation and functions [16,17], and stimulates the production of pro-inflammatory cytokines including interleukin (IL)-1α, IL-1β, IL-6, IL-8, IL-18 and tumor necrosis factor (TNF)-α in monocytes [18]. Periodontitis is influenced by systemic diseases such as DM, HIV/AIDS, and osteoporosis [19]. DM is a risk factor for periodontitis and DM-associated periodontitis exhibits more extensive and severe bone destruction and gingival inflammation than non-DM periodontitis [20,21]. Advanced glycation end-products (AGEs) are formed in the chronic hyperglycemia of DM and are associated with incidence of some DM complications, Alzheimer's disease, sarcopenia, and arthritis [22,23]. AGEs bind to the receptor of AGEs (RAGE) and increase reactive oxygen species (ROS) activity, vascular inflammation, macrophage and platelet activation, and the migration of inflammatory cells [24]. Furthermore, pentosidine, which is an AGE, has been shown to accumulate in cortical and trabecular bones and weaken bone strength [25].

AGEs accumulate in the gingival tissues of patients with DM and periodontitis [26], up-regulate the expression of inflammatory mediators, such as IL-1β, IL-6, and TNF-α, in periodontal tissues, and inhibit bone nodule formation by osteoblasts [27,28]. A previous study reported that AGEs decreased alkaline phosphatase (ALPase) activity and bone nodule formation by bone marrow cells and also inhibited osteoblastic cells differentiation [29]. These findings show that AGEs aggravate bone formation as well as inflammation in periodontal tissues in DM-associated periodontitis. On the other hands, sclerostin levels were found to be increased in the serum and periodontal tissues of patients with periodontitis [30], and its levels in the gingival crevicular fluid from inflamed periodontal sites was higher than that from healthy sites [31], suggesting that sclerostin influences periodontal conditions with gingival inflammation and alveolar bone resorption.

Although AGEs and *P*-LPS are important factors in periodontitis and DM, their effects on osteocytes in periodontitis with DM remain unclear. To clarify alveolar bone metabolism in DM-associated periodontitis, the effects of AGEs and *P*-LPS on sclerostin expression in osteocytes and sclerostin function for osteoblastic cells were investigated.

2. Materials and methods

2.1. Preparation of AGEs (AGE2)

AGEs (AGE2) were prepared as previously described by Okazaki et al. [32]. In brief, 50 mg/ml bovine serum albumin (BSA; Sigma-Aldrich, St. Louis, MO, USA) was incubated with 0.1 M DL-glyceraldehyde (Sigma-Aldrich) under sterile conditions in 0.2 M phosphate buffer (pH 7.4) at 37 °C for 7 days, and then dialyzed against phosphate-buffered saline (pH 7.4) for three days. Non-glycated BSA was prepared under similar conditions without DL-glyceraldehyde. The fluorescence strength of AGEs solution was 40-fold greater than that of BSA at an excitation/emission wavelength of 370/440 nm.

2.2. Cell cultures

Mouse osteocyte-like MLO-Y4-A2 cells were kindly provided by Prof. T Sugimoto (Shimane University) with the consent of Prof. Lynda F Bonewald (Indiana University). MLO-Y4-A2 cells were seeded at 5000 cells/cm^2 on type I collagen-coated dishes (IWAKI, Tokyo, Japan), and cultured in α-Eagle's minimum essential medium (α-MEM) containing 10% fetal bovine serum (FBS) and antibiotics (100 U/ml penicillin G, 50 μg/ml streptomycin, Meiji, Tokyo, Japan) at 37 °C in a humidified atmosphere containing of 95% air and 5% CO_2. Medium was changed every two days. On day 5, cells were reached subconfluency and were cultured with 100 μg/ml AGEs and 250 ng/ml *P*-LPS (WAKO, Osaka, Japan) for 24–48 h.

2.3. Assessment of cell viability

MLO-Y4-A2 cells were cultured in growth medium (α-MEM-10% FBS) for 5 days, cultured with AGE2, BSA and *P*-LPS for 48 h, and then incubated further in culture medium containing Cell Counting Kit-8 solution (Dojindo Laboratories, Kumamoto, Japan) for 4 h. The absorbance of the culture medium was measured at a wavelength of 450 nm to evaluate cell viability.

2.4. RNA isolation and real-time PCR

Total RNA was prepared from cultured cells using the RNeasy Mini kit (QIAGEN, Hilden, Germany) and cDNA was synthesized using the Prime Script II 1st strand cDNA Synthesis Kit (TAKARA Bio, Shiga, Japan). The sequences of the primers (forward/reverse) used were as follows: SOST: 5′-TACCCTCGCCGGACCTATAC-3′ and 5′-CAGGTCAGG GTC AGAAACCC-3′, RAGE: 5′-AGGAACGTGCAGAGCTGAAT-3′ and 5′-CTGGTTGGA GAAGGAAGTGC-3′, TLR2: 5′-TGCTTTCCTGCTGAAGATTT-3′ and 5′-TGTACCGCA ACAGCTTCAGG-3′, IL-6: 5′-GAGGATACC ACTCCCAACAGACC-3′ and 5′-AAGTGCATCATCGTTGTTCATACA-3′, Runx2: 5′-ACTATGGCGTCAAACAGCCT-3′ and 5′-GGTGCTCGGATCCCAAAAGA-3′, GAPDH: 5′-GTGTTCCTACCCCCAATGTG-3′ and 5′-AGGAGA CAACCTGGTCCTCA-3′. All PCR amplifications were performed using the CFX96 Touch Real-Time PCR Detection System (Bio-Rad, Hercules, CA, USA) with SsoAdvanced Universal SYBER Green Supermix (Bio-Rad) according to the manufacturer's instructions. mRNA expression levels were normalized against the GAPDH gene.

2.5. Enzyme-linked immunosorbent assay (ELISA)

Sub-confluent MLO-Y4-A2 cells were incubated with AGE2 (100 μg/ml), BSA (100 μg/ml) and *P*-LPS (250 ng/ml) for 48 h. Sclerostin and IL-6 protein levels in cultured medium were measured using ELISA kit (R&D systems, Minneapolis, MN, USA) according to the manufacturer's instructions.

2.6. Western blotting

Sub-confluent osteocytes were cultured with AGE2 (100 μg/ml) and *P*-LPS (250 ng/ml) for 48 h for a Western blot analysis of RAGE and TLR2. In another experiment to examine signaling pathways, osteocytes were treated with AGE2 and *P*-LPS for 1 h. Treated cells were prepared using the RIPA Lysis Buffer system containing protease inhibitor cocktail and sodium orthovanadate (Santa Cruz Biotechnology, Santa Cruz, CA, USA), and were centrifuged at 14,000*g* for 15 min at 4 °C. Total protein in the supernatants was measured using BCA Protein Assay kit (TAKARA Bio, Japan). Extracted protein (30 μg of total protein) was electrophoretically separated on SDS-polyacrylamide gels (10%) and transferred to polyvinylidene difluoride (PVDF) membranes (Amersham Hybond P PVDF membrane, GE Healthcare Japan, Tokyo, Japan). After blocking with PVDF Blocking Reagent for Can Get Signal (TOYOBO, Osaka, Japan) for 1 h at room temperature, membranes were reacted with an anti-RAGE antibody (Ab) (1/1000 dilution, Abcam plc, Cambridge, UK), mouse monoclonal anti-TLR2 Ab (1/250 dilution, Abcam), and anti-p38 MAPK Ab, anti-phospho-p38 MAPK Ab, anti-JNK Ab, anti-phospho-JNK Ab, anti-ERK 1/2 Ab, anti-phospho-ERK 1/2 Ab, anti-p65-NF-κB Ab, anti-phospho-p65-NF-κB Ab, and anti-β-actin Ab (1/1000–1/20,000 dilution, Cell Signaling Technology, Danvers, MA, USA) at 4 °C overnight. In Western blotting of β-catenin, the membrane was reacted with an anti-β-catenin and anti-phospho-β-catenin Abs (1/1000 dilution, Cell Signaling Technology) at 4 °C overnight. After membranes had been washed with 0.1% Tween 20 in Tris-buffered

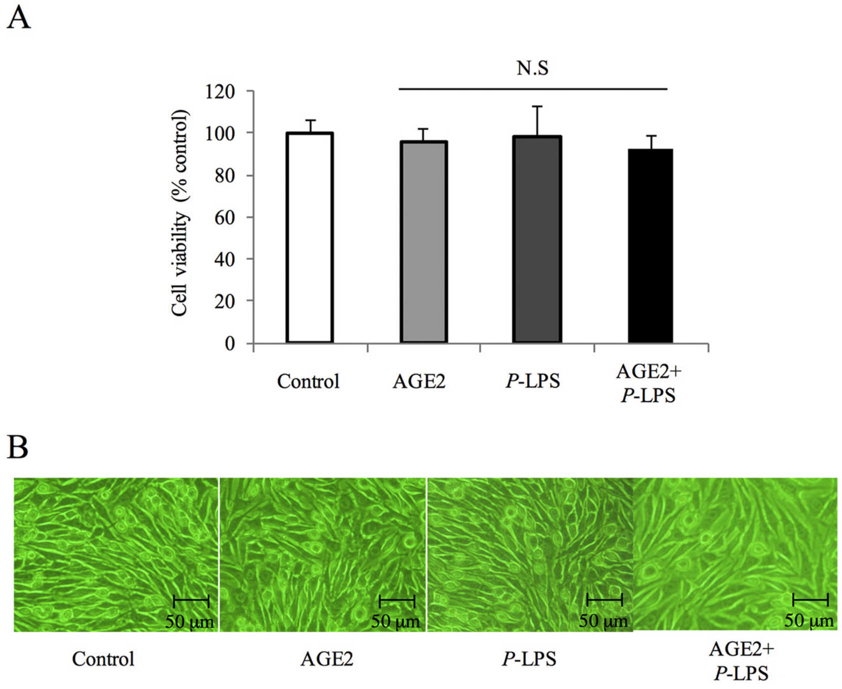

Fig. 1. Effects of AGE2 and *P*-LPS on the cell viability of osteocytes. (A) MLO-Y4-A2 cells were seeded at 5000 cells/cm^2, cultured for 5 days, and then cultured with BSA (100 μg/ml; Control), AGE2 (100 μg/ml), and *P*-LPS (250 ng/ml) for 48 h. Cell viability was assessed using Cell Counting Kit-8®. Data are expressed as mean ± SD of quadruplicate cultures (n = 4). N.S shows no significant differences from the control group with BSA. (B) Cell morphology was observed with phase-contrast microscopy after cultures with BSA (100 μg/ml; control), AGE2 (100 μg/ml), and *P*-LPS (250 ng/ml) for 48 h. (Magnification ×100).

saline (TBS), they were reacted with horseradish peroxidase (HRP) conjugate mouse anti-rabbit IgG or HRP conjugate rabbit anti-mouse IgG (1/2000 dilution, Cell Signaling Technology) for 1 h at room temperature, and then developed by Amercham ECL Western Blotting Detection Reagents (GE Healthcare Japan) and visualized using Image Quant LAS 500 (GE Healthcare Japan).

2.7. siRNA transfection

Osteocytes were seeded at 5000 cells/cm^2 on collagen-coated dish and cultured for 4 days in culture medium. When cells were 60–80% confluent, the mouse siRNAs (50 nM) of RAGE (QIAGEN), TLR2 (QIAGEN), and control siRNA (Santa Cruz Biotechnology) were transfected into osteocytes using Lipofectamin RNAiMax (Thermo Fisher, Waltham, MA, USA) according to the manufacturer's instructions. After transfection for 24 h, osteocytes were treated with AGE2 (100 μg/ml) and *P*-LPS (250 ng/ml) for 24–48 h, and used for quantitative real-time PCR and ELISA to measure sclerostin levels.

2.8. Inhibition of MAPK and NF-κB signaling pathways

Sub-confluent osteocytes were pre-treated with specific inhibitors of p38 (SB203580, 20 μM), JNK (SP600125, 20 μM), and ERK1/2 (U0126, 10 μM) for 1 h, and with Iκ-Bα inhibitors (Bay11-7082, 5 μM) for 24 h. After the pretreatment with the inhibitors, osteocytes were cultured with AGE2 (100 μg/ml) and *P*-LPS (250 ng/ml) for 24–48 h and used to measure sclerostin levels.

2.9. Co-culture system and ALPase activity measurements

The function of sclerostin secreted from osteocyte-like cells during osteoblast differentiation was investigated using a sclerostin-neutralizing antibody and co-culture system of osteocytes (MLO-Y4-A2 cells) and osteoblastic cells (MC3T3-E1 cells). For preliminary experiment, the effective concentration of sclerostin-neutralizing antibody on SOST expression in culture of osteocyte-like cells. In brief, MLO-Y4-A2 cells were seeded at a density of 5000 cells/cm^2 on type I collagen-coated culture inserts (Corning, NY, USA) and cultured for 5 days until sub-confluent. Osteocytes were cultured with AGE2 (100 μg/ml) and *P*-LPS (250 ng/ml) for 48 h and further cultured with a sclerostin-neutralizing antibody (1–10 μg/ml, AbD09097-h/m IgG2a, Bio-Rad) for 24 h. Cultured medium was used to assess sclerostin concentrations with the ELISA kit for sclerostin. In the co-culture experiment, MLO-Y4-A2 cells were seeded at a density of 5000 cells/cm^2 on type I collagen-coated culture inserts (Corning, NY, USA), cultured for 5 days until sub-confluent, and further pre-treated with AGE2 (100 μg/ml) and *P*-LPS (250 ng/ml) for 48 h. MC3T3-E1 cells were seeded at a density of 30,000 cells/ml, cultured in α-MEM-10% FBS for 3 days, and then cultured in differentiation medium (α-MEM-10%FBS containing 50 μg/ml ascorbic acid and 2 mM β-glycerol phosphate) for 4 days. Pre-treated osteocytes in the culture insert and osteoblastic cells in the outer well were co-cultured in medium containing the sclerostin-neutralizing antibody, but not AGE2 or *P*-LPS for 24 h. After the co-culture, osteoblastic cells were scraped into 50 mM Tris-HCl buffer (pH = 7.4), sonicated and centrifuged at 2000 ×*g* for 10 min. ALPase activity in the supernatant was determined using *p*-nitrophenyl phosphate as the substrate according to Lowry's methods [33]. The total protein content in the cellular fraction was measured using Bio-Rad protein assay reagent (Bio-Rad) and ALPase activity was normalized by the total amount of protein. Data were shown as a ratio to control BSA (%).

2.10. Statistical analysis

All experiments were performed more than three times to verify results and the data obtained from a typical experiment were expressed as the mean ± SD (n = 3 or 4). Data in real-time PCR was analyzed using total nine RNA samples in three separated experiments. Statistical comparisons among control and experimental groups were performed by ANOVA and the significance of differences was estimated by *post-hoc* testing using the Turkey-Kramer method. A Student *t*-test was used for pairwise comparisons. All analyses were performed with Stat view v.5.0 (SAS Institute Inc. Cary, NC, USA). $P < 0.05$ was considered to be significant.

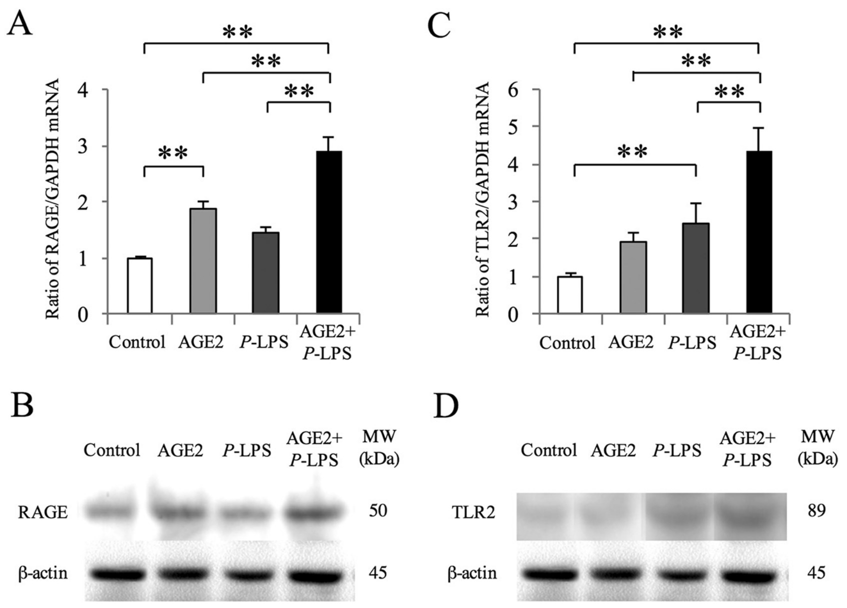

Fig. 2. Effects of AGE2 and *P*-LPS on the expression of RAGE and TLR2 in osteocytes. (A and C) Total RNA was isolated from MLO-Y4-A2 cells treated with BSA (100 μg/ml; Control), AGE2 (100 μg/ml), and *P*-LPS (250 ng/ml) for 24 h. The expression of RAGE and TLR2 mRNAs was analyzed by quantitative RT-PCR using specific primers, and normalized by GAPDH mRNA expression. Data are expressed as the mean ± SD of triplicate cultures in three separated experiments (total 9 samples). Asterisks show a significant difference ($^{**}P < 0.01$). (B and D) Cell lysate samples were prepared from osteocytes cultured with BSA (100 μg/ml; Control), AGE2 (100 μg/ml), and *P*-LPS (250 ng/ml) for 48 h. RAGE, TLR2, and β-actin proteins in cell lysates were assayed by Western blotting using each specific antibody.

3. Results

3.1. Effects of AGE2 and P-LPS on the viability of MLO-Y4-A2 cells

After MLO-Y4-A2 cells were cultured with AGE2 (100 μg/ml) and *P*-LPS (250 ng/ml) for 48 h, the viability of osteocytes was not significantly changed (Fig. 1A), and cellular morphology was not altered (Fig. 1B).

3.2. Effects of AGE2 and P-LPS on the expression of RAGE and TLR2

The expression of RAGE and TLR2 in osteocytes cultured with AGE2 (100 μg/ml) and *P*-LPS (250 ng/ml) for 24–48 h were investigated. AGEs significantly increased the expression of RAGE mRNA (Fig. 2A). Although *P*-LPS did not significantly increase RAGE levels, the co-stimulation with AGE2 and *P*-LPS elevated RAGE levels more than AGE2 alone. RAGE protein levels in osteocytes were increased by AGE2 as well as AGE2 and *P*-LPS (Fig. 2B).

P-LPS significantly elevated TLR2 mRNA levels in osteocytes, and these levels increased further when osteocytes were cultured with *P*-LPS and AGE2; however, AGE2 alone did not significantly increase TLR2 levels (Fig. 2C). TLR2 protein levels in osteocytes appeared to be increased by *P*-LPS as well as by the combination of AGE2 and *P*-LPS (Fig. 2D).

3.3. Effects of AGE2 and P-LPS on the expression of sclerostin and IL-6

AGE2 (100 μg/ml) significantly increased sclerostin mRNA and protein levels in osteocytes (Fig. 3A and B). *P*-LPS (250 ng/ml) also significantly increased sclerostin mRNA and protein levels, and *P*-LPS and AGE2 further elevated sclerostin levels over those with AGE2 or *P*-LPS alone. AGE2 and *P*-LPS increased IL-6 mRNA and protein expression levels, similar to sclerostin expression levels, and the combination of AGE2 and *P*-LPS significantly increased IL-6 levels over those with AGE2 or *P*-LPS alone (Fig. 3C and D).

When the effects of AGE2 and *P*-LPS on sclerostin expression were investigated in another osteocytic cell line, IDG-SW3 cells, the expressions of sclerostin mRNA and protein were increased by AGE2 and *P*-LPS, and the further elevation was observed in the culture with combination of AGE2 and *P*-LPS (Supplementary Fig. 1).

3.4. Effect of RAGE and TLR2 siRNAs on sclerostin expression

To investigate the signal pathways of AGE2- and *P*-LPS-induced sclerostin expression, the effects of siRNAs of RAGE and TLR2 were investigated. The siRNAs of RAGE and TLR2 significantly inhibited RAGE and TLR2 mRNA expression, respectively (Fig. 4A and D), but did not influence TLR2 and RAGE mRNA expression, respectively (Supplementary Fig. 2). The siRNA of RAGE significantly decreased AGEs-induced sclerostin and RAGE expressions as well as AGE2 and *P*-LPS-induced sclerostin and RAGE expressions in osteocytes (Fig. 4B: SOST mRNA, Fig. 4C: sclerostin protein, Supplementary Fig. 2C: RAGE mRNA, Supplementary Fig. 2G: RAGE protein), however, did not show significant decrease of TLR2 mRNA expression (Supplementary Fig. 2D). When the TLR2 gene was knocked down by its siRNA, *P*-LPS- and AGE2 and *P*-LPS-induced sclerostin and TLR2 expressions was significantly inhibited by TLR2 siRNA (Fig. 4E: SOST mRNA, Fig. 4F: sclerostin protein, Supplementary Fig. 2F: TLR2 mRNA, Supplementary Fig. 2G: TLR2 protein). In contrast, *P*-LPS did not significantly increase RAGE mRNA expression in osteocyte-like cells transfected with siControl and siTLR2 (Supplementary Fig. 2E).

3.5. Relationship with MAPKs and NF-κB in AGE2- and P-LPS-induced sclerostin expression

Analysis of MAPK phosphorylation in osteocytes showed that AGE2 stimulated the phosphorylation of the MAPKs of JNK and ERK, and further enhanced p65 NF-κB phosphorylation (Fig. 5A). *P*-LPS increased the phosphorylation of p38, JNK, and p65. The co-stimulation with AGE2 and *P*-LPS increased the phosphorylation of p38, JNK, and p65 more than with AGE2 or *P*-LPS alone. The JNK inhibitor (SP600125) and ERK inhibitor (U0126) significantly decreased AGEs-induced sclerostin expression levels (Fig. 5B: SOST mRNA, Fig. 5C: sclerostin protein). On the other hand, *P*-LPS-stimulated sclerostin expression was inhibited by the p38 inhibitor (SB203580) and JNK inhibitor. Inhibitors of MAPKs, including p38, JNK and ERK, significantly reduced AGEs and *P*-LPS-induced increases in sclerostin expression.

AGE2 and *P*-LPS stimulated the phosphorylation of p65 NF-κB, and the co-stimulation with AGE2 and *P*-LPS further enhanced p65 phosphorylation (Fig. 5A). The NF-κB inhibitor (BAY11-7082) significantly decreased AGE2-, *P*-LPS- and their combination-induced sclerostin expression (Fig. 5D: SOST mRNA, Fig. 5E: sclerostin protein).

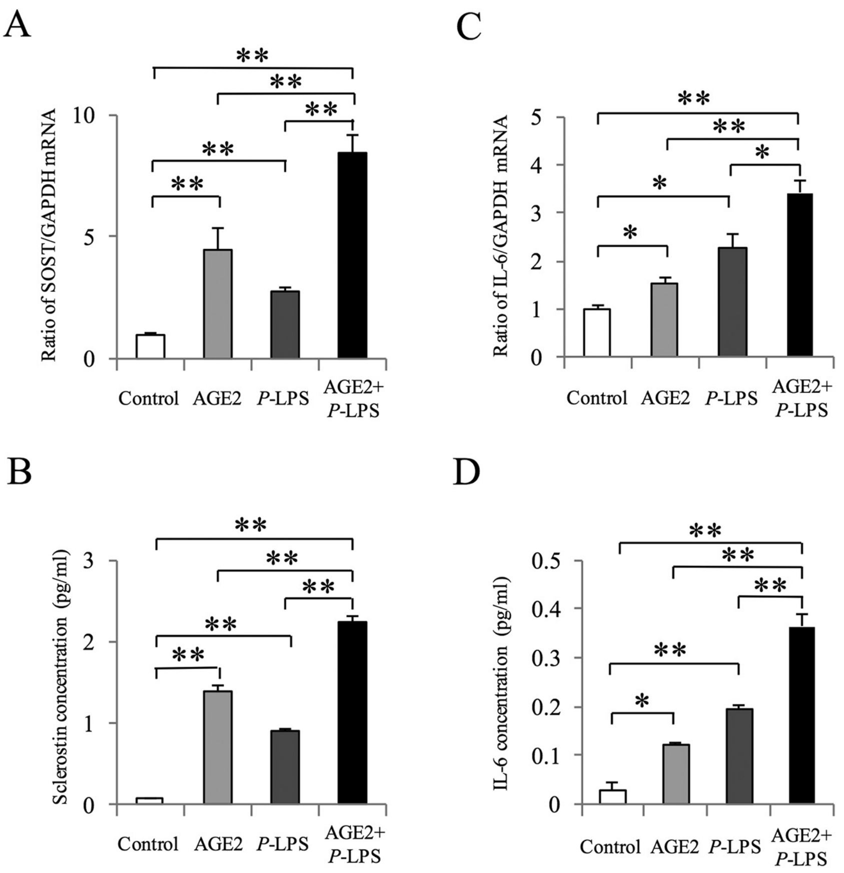

Fig. 3. Effects of AGE2 and *P*-LPS on the expression of sclerostin and IL-6 in osteocytes. MLO-Y4-A2 cells were cultured with BSA (100 μg/ml; Control), AGE2 (100 μg/ml), and *P*-LPS (250 ng/ml) for 24–48 h after becoming sub-confluent. (A and C) Total RNA was isolated from osteocytes treated with BSA, AGE2, and *P*-LPS for 24 h, and SOST and IL-6 mRNA expression was assessed by quantitative RT-PCR. SOST and IL-6 mRNA expression was normalized by GAPDH mRNA expression. (B and D) Osteocytes were cultured with BSA (Control), AGE2, and *P*-LPS for 48 h, and sclerostin and IL-6 levels in the supernatant were measured using each ELISA kit. Data are expressed as the mean ± SD of triplicate cultures in three separated experiments (total 9 samples). Asterisks show a significant difference (*$P < 0.05$, **$P < 0.01$).

3.6. *Effects of AGE2 and P-LPS on the ALPase activity of osteoblastic cells in the co-culture system*

When phosphorylated β-catenin was analyzed in osteoblastic cells that were co-cultured with osteocyte-like cells pre-treated with AGE2, *P*-LPS and AGE2 and *P*-LPS in order to examine the association between sclerostin derived from osteocyte-like cells and Wnt signal in osteoblastic cells, the expression of phosphorylated β-catenin was increased by AGE2 and *P*-LPS (Fig. 6A). Furthermore, AGE2 and *P*-LPS caused more expression of β-catenin in osteoblastic cells.

The function of sclerostin induced by AGE2 and *P*-LPS was investigated using the co-culture system with osteocytes (MLO-Y4-A2 cells) and osteoblastic cells (MC3T3-E1 cells). When the effective concentration of sclerostin-neutralizing antibody was investigated, 1–10 μg/ml of sclerostin-neutralizing antibody significantly inhibited AGEs-induced sclerostin expression in osteocytes (Fig. 6B). When osteoblastic cells were co-cultured with osteocytes pre-cultured with AGE2 and *P*-LPS for 24 h, ALPase activity in osteoblastic cells was significantly inhibited (Fig. 6C). ALPase activity further decreased in osteoblastic cells co-cultured with osteocytes that were co-stimulated with AGE2 and *P*-LPS. The sclerostin-neutralizing antibody (2 μg/ml) slightly decreased the inhibition of ALPase activity in osteoblastic cells that were co-cultured with osteocytes treated with AGE2 or *P*-LPS only, and significantly recovered ALPase activity inhibited by AGE2 and *P*-LPS (Fig. 6C). When the expression of Runx2 mRNA in osteoblastic cells co-cultured with osteocyte-like cells that were pre-treated with AGE2, *P*-LPS and AGE2 and *P*-LPS was investigated using a sclerostin-neutralizing antibody, its antibody significantly decreased *P*-LPS- and AGE2 and *P*-LPS-induced the inhibition of Runx2 expression in osteoblastic cells (Fig. 6D).

4. Discussion

Periodontal diseases in DM patients are aggravated by high glucose conditions and AGEs, which affect bone metabolism as well as inflammation in periodontal tissues [34–36]. The present study showed that AGE2 up-regulated the expression of sclerostin, which is known to reduce bone formation and shows elevated serum levels in DM patients [4,9,10]. AGEs inhibited type I and type III collagen synthesis and increased matrix metalloproteinase-1 expression in human gingival fibroblasts [37,38], and increased IL-1β expression and decreased ALPase activity and bone nodule formation in osteoblastic cells derived from bone marrow [29], suggesting the pathological effects of AGEs on inflammation and the destruction of periodontal tissues in DM. Few studies have examined the regulation and mechanism underlying AGEs- and LPS-induced sclerostin expression. Tanaka et al. [39] reported that AGE2/AGE3 increased sclerostin protein expression levels in osteocytes by approximately two-fold. AGE3 increased sclerostin expression and apoptosis by up-regulating TGF-β expression in osteocytes [40]. In the present study, AGEs (AGE2) and *P*-LPS up-regulated sclerostin protein levels in osteocyte-like cells (MLO-Y4-A2 cells) by approximately 19- and 12-fold, respectively, and the combination of AGEs and *P*-LPS synergistically increased sclerostin expression levels to approximately 30-fold those of control. Furthermore, AGE2 and *P*-LPS significantly increased sclerostin expression in another osteocyte-like cell line (IDG-SW3 cells, Supplementary Fig. 1). Sclerostin levels in GCF from periodontal diseases sites were significantly higher than those from healthy sites [31], and the resorption of alveolar bone and number of sclerostin-positive osteocytes were higher in rats with streptozotocin-induced DM and ligature-induced periodontitis than in non-DM, periodontitis rats [41]. These result and reports suggest that AGEs (AGE2) and *P*-LPS may cause a catabolic action on alveolar bone metabolism through sclerostin pathway in periodontitis of DM patients.

AGEs and *P*-LPS increased the expression of IL-6 as well as sclerostin

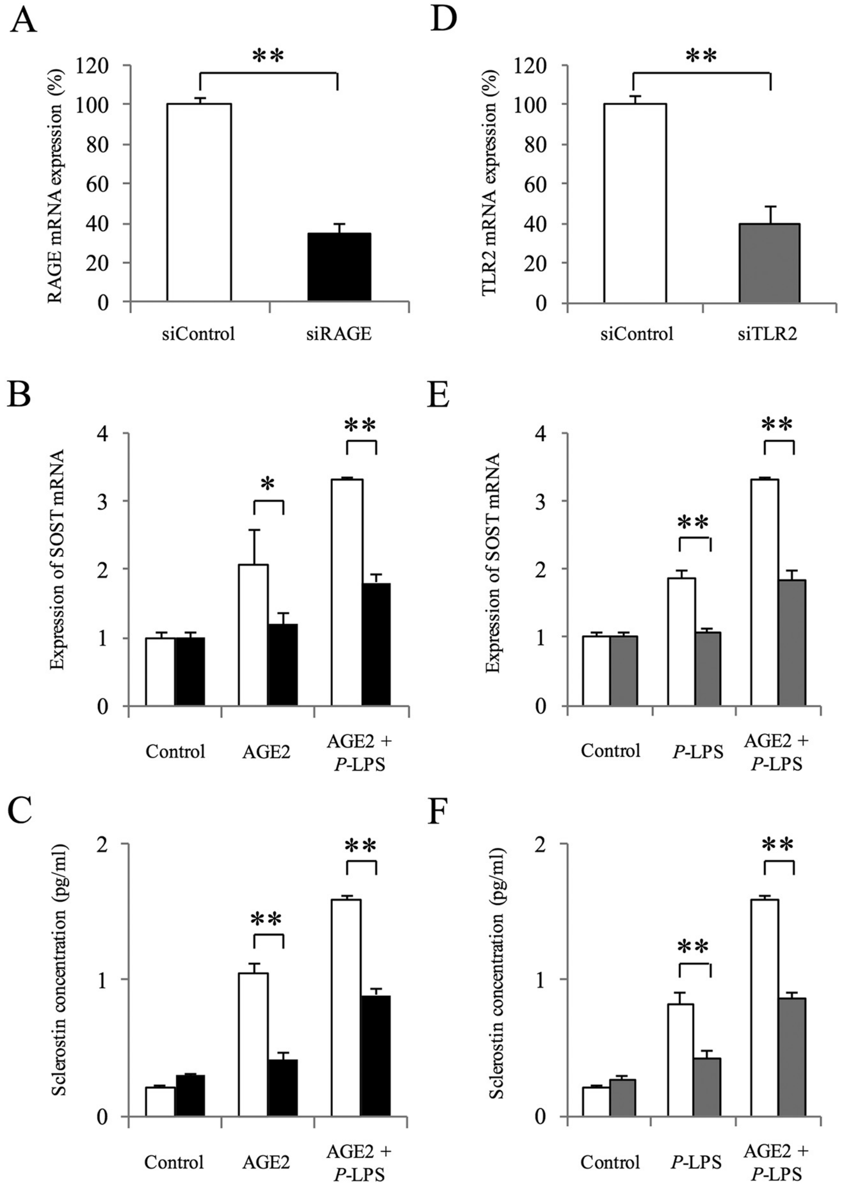

Fig. 4. Effects of RAGE and TLR2 knockdown on AGE2- and *P*-LPS-induced sclerostin expression in osteocytes. When MLO-Y4-A2 cells reached 70% confluency, they were transfected with negative control siRNA (siControl, 10 and 50 μmol/l), RAGE siRNA (siRAGE, 50 μmol/l), and TLR2 siRNA (siTLR2, 10 μmol/l) for 24 h. Osteocytes transfected with siRNAs were cultured with BSA (100 μg/ml; Control), AGE2 (100 μg/ml), and *P*-LPS (250 ng/ml) for 24–48 h. (A and D) Total RNA was isolated from cells transfected siRNAs, and RAGE and TLR2 mRNA expression was assessed by quantitative RT-PCR. Osteocytes were transfected with siControl (open column), siRAGE (closed column), and siTLR2 (hatched column), and then stimulated by BSA, AGE2, and *P*-LPS. Sclerostin mRNA and protein levels in transfected osteocytes were measured using quantitative RT-PCR (B and E) and ELISA (C and F), respectively. Data are expressed as the mean ± SD of triplicate cultures in three separated experiments (total 9 samples). Asterisks show a significant difference ($^*P < 0.05$, $^{**}P < 0.01$).

in osteocyte-like cells, and the combination of these two factors resulted in further increase in IL-6 levels than those with AGEs or *P*-LPS alone. AGEs up-regulated IL-6 and VEGF expression and induced apoptosis by activating the ERK, p38, and STAT3 pathways in MLO-Y4 cells [42], and increased IL-6 and ICAM-1 expression in human gingival fibroblasts [43]. On the other hand, *P*-LPS increased IL-6 expression in periodontal ligament stem cells and inhibited osteoblastic differentiation [44]. IL-6 expression levels in periodontal tissues were higher in patients with DM-associated periodontitis than in those with periodontitis [45]. AGEs and *P*-LPS appear to induce inflammation and bone metabolism by IL-6 and sclerostin in periodontal tissues, and aggravate periodontitis in DM patients.

Osteocyte-like cells of the MLO-Y4 cell line express RAGE, and the expression of which was increased by AGEs [42], while RAGE expression in MLO-Y4-A2 cells was up-regulated by AGE2 and further enhanced by AGE2 and *P*-LPS, but not significantly by *P*-LPS alone in the present study (Fig. 2). On the other hand, the knockdown of TLR2 mRNA decreased AGE2 and *P*-LPS-induced RAGE expression (Supplementary Fig. 2). LPS from *Escherichia coli* binds to RAGE in neutrophils and monocytes [46], and RAGE levels increased when murine aortic endothelial cells were infected with *P. gingivalis* [47]. However, an interaction between RAGE and TLR2 was not well known. Although the effect of *P*-LPS on RAGE expression in osteocyte-like cells was very weak, TLR2 may regulates RAGE expression and its signaling pathway. Regarding TLR2, mouse parietal osteoblasts expressed *Tlr2*, and *P*-LPS stimulated RANKL by increasing TLR2 expression in osteoblasts [48]. *P. gingivalis* up-regulated TLR2 expression in bone marrow cells and inhibited the RANKL-induced differentiation of osteoclasts derived from bone marrow cells [49]. Although TLR2 has been detected in osteoblasts, osteoclasts, and mesenchymal stem cells [50], it was not found in osteocytes. The present study is the first to show TLR2 in osteocytes, and that its expression was increased by *P*-LPS and enhanced further by the combination of *P*-LPS and AGE2. In contrast, significant change in TLR2 expression by AGE2 treatment and knockdown of RAGE was not observed (Fig. 2 and Supplementary Fig. 2). However, AGE2 and *P*-LPS synergistically increased sclerostin and IL-6 expressions by up-regulating RAGE and TLR2 expressions. The reasons for these synergistic increases in sclerostin and IL-6 have not yet been elucidated in detail. When normal human bone-derived cells were cultured with TNF-α, SOST mRNA expression levels increased [51]. AGE2 and *P*-LPS also increased the mRNA expression of TNF-α as well as IL-6 in the osteocytes used in the present study (Supplementary Fig. 3). AGEs (AGE2)

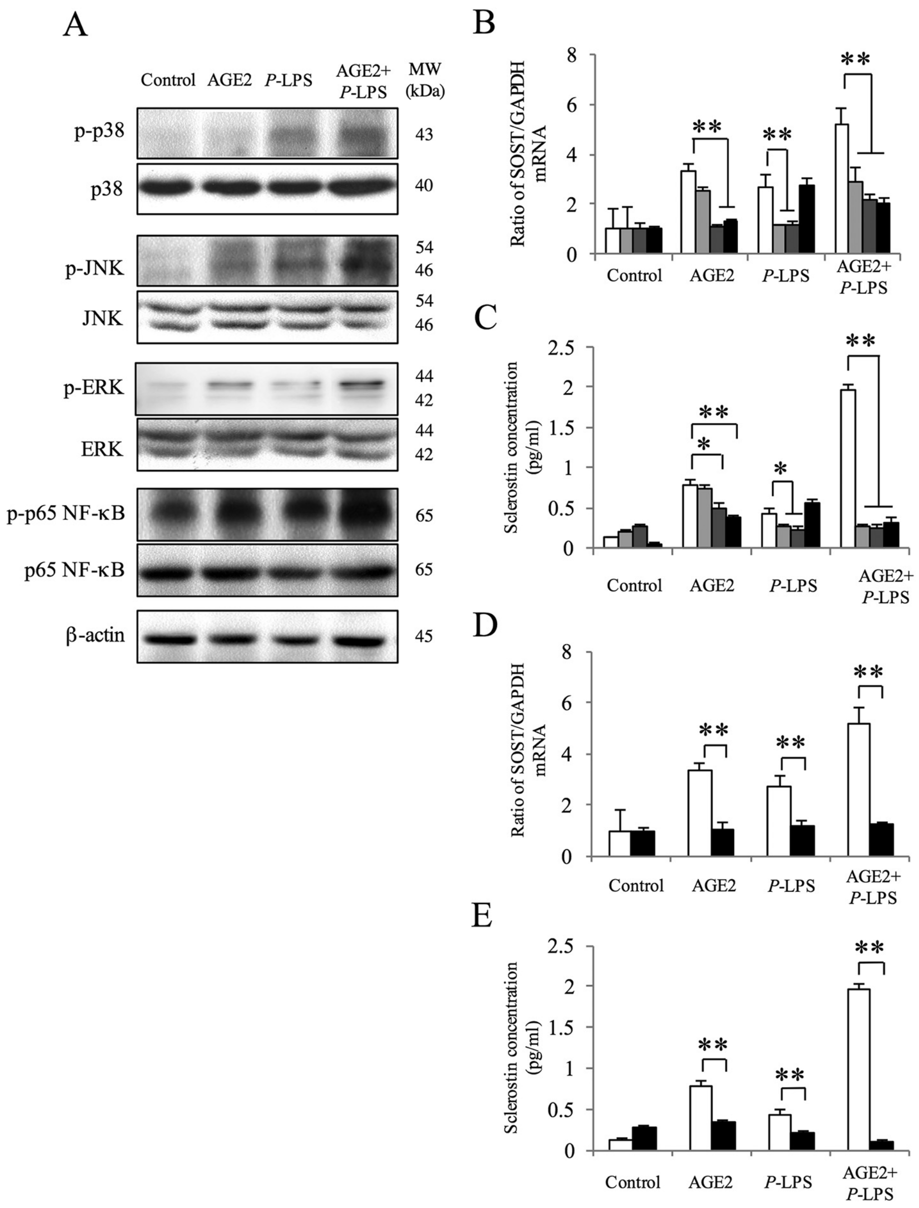

Fig. 5. Effects of AGE2 and *P*-LPS on the phosphorylation of MAPKs and NF-κB, and inhibitors on AGE2- and *P*-LPS-induced sclerostin expression. (A) Sub-confluent MLO-Y4-A2 cells were treated with BSA (100 μg/ml; Control), AGE2 (100 μg/ml), and *P*-LPS (250 ng/ml) for 60 min, and cell lysate samples were prepared. The phosphorylation of MAPKs and NF-κB was analyzed by Western blotting using antibodies for p38, phospho-p38, JNK, phospho-JNK, ERK, phospho-ERK, p65 NF-κB, and phospho-p65 NF-κB. (B–E) Osteocytes were pre-treated with SB203580 (30 μM, dotted column), SP600125 (20 μM, diagonal striped column), and U0126 (10 μM, closed column) for 1 h, and Bay11-7082 (5 μM, horizontal striped column) for 24 h, and then cultured with AGEs (100 μg/ml) and *P*-LPS (250 ng/ml) for 24–48 h. The expression of SOST mRNA was assessed by quantitative RT-PCR (B and D), and sclerostin protein levels in the supernatant were measured by ELISA (C and E). Data are expressed as the mean ± SD of triplicate cultures in three separated experiments (total 9 samples). Asterisks show a significant difference (*$P < 0.05$, **$P < 0.01$).

directly increase sclerostin expression via the RAGE pathway, and *P*-LPS may indirectly up-regulate sclerostin expression by inducing the expression of IL-6 and other cytokines in osteocytes. Therefore, AGEs and *P*-LPS may induce greater increases in sclerostin expression levels in combination than alone via direct and indirect pathways. However, an exact interaction between RAGE and TLR2 was not elucidated in the present study.

The signaling pathways of AGEs-induced sclerostin expression in osteocytes currently remain unclear. AGEs increased IL-6 and VEGF expressions levels via the ERK, p38, and STAT3 signal pathways in osteocytes of MLO-Y4 cells line [42], and activated the phosphorylation of ERK, JNK, and NF-κB, while their inhibitors significantly decreased AGE2-induced sclerostin expression in MLO-Y4-A2, a sub-cloned of MLO-Y4 cells, in the present study. AGEs mediated the proliferation of human fetal osteoblastic cells by stimulating the RAGE, Raf/MEK/ERK signal pathway [52], increased RAGE expression, activated NF-κB, and regulated the proliferation and function of human osteoblasts [53]. AGEs influence the growth and function of osteocytes and osteoblasts via the signal pathways of RAGE, MAPK, and their transcription factors, and affect alveolar bone metabolism in periodontitis with DM. On the other hand, *P*-LPS up-regulated sclerostin expression via the TLR2, JNK, p38, and NF-κB signal pathways in osteocytes. The signal pathway of *P*-LPS-stimulated sclerostin expression remains nuclear because the relationship between sclerostin and *P*-LPS has not yet been examined. Although AGEs (AGE2) and *P*-LPS activated NF-κB, the MAPK signaling pathway differed between ERK and p38. The stimulation of each kinase may induce further increases sclerostin expression by AGEs and *P*-LPS administered in combination than alone.

Sclerostin inhibits canonical Wnt signaling, which regulates osteoblastic cells differentiation and bone formation [54], and suppresses the proliferation and function of osteoblast [55]. Wnt antagonists such as Dkk1 and sclerostin phosphorylate β-catenin and it is ubiquitinated and degraded by proteasome [56]. β-Catenin in MC3T3-E1 cells was phosphorylated in our co-culture system, and this result suggests that AGE2- and *P*-LPS-induced sclerostin inhibits Wnt signaling in osteoblasts.

Rats with DM showed lower bone mass density (BMD) of femoral and spinal, and the sclerostin-neutralizing antibody further inhibited their BMD [57]. Sclerostin inhibited bone morphogenetic protein (BMP) signaling by competing with binding between BMP and its receptor, and suppressed the mineralization of osteoblastic cells [58], and a sclerostin antibody inhibited LPS-induced reductions of peri-implant bone volume via the Wnt signaling pathway [59]. Furthermore, when

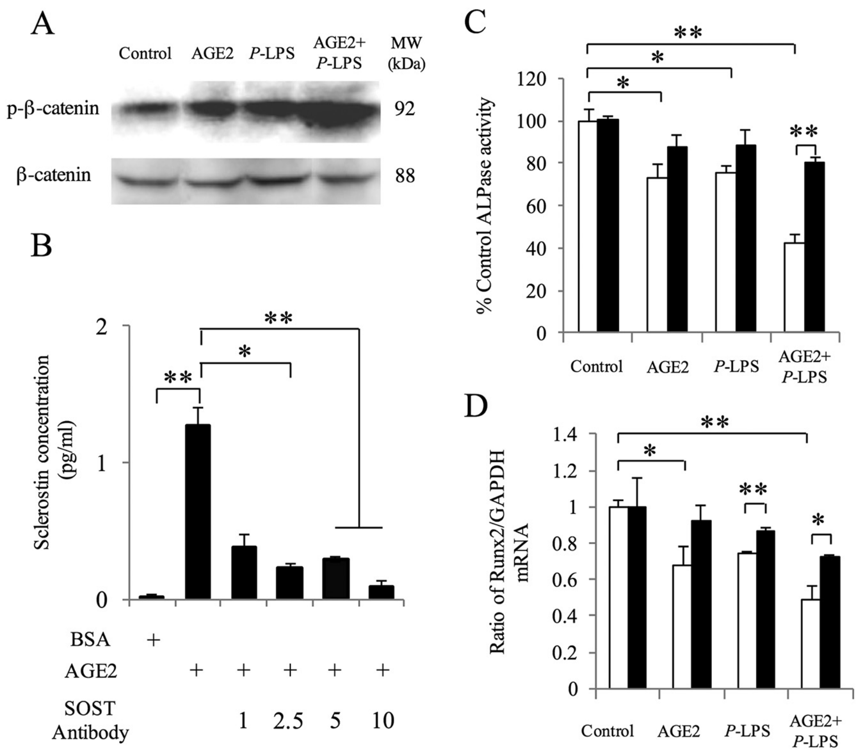

Fig. 6. Effects of AGE2 and *P*-LPS on the ALPase activity of osteoblastic cells in a co-culture system with osteocytes and osteoblastic cells. (A) Osteocytes were cultured with BSA (100 μg/ml; Control), AGE2 (100 μg/ml), and *P*-LPS (250 ng/ml) for 48 h, and transferred to a culture insert of the co-culture system. Osteoblastic cells were pre-cultured in medium containing ascorbic acid (50 mg/ml) and β-glycerol phosphate (2 mM) in the outer culture well. Osteoblastic cells were co-cultured with pre-treated osteocytes for 24 h, and cell lysate samples were prepared from osteoblastic cells. Phosphorylation of β-catenin was analyzed by Western blotting. (B) MLO-Y4-A2 cells were pre-cultured with AGE2 (100 μg/ml) and BSA (100 μg/ml) for 48 h, and then cultured with a sclerostin- neutralizing antibody (1–10 μg/ml) for 24 h. Sclerostin protein levels in the supernatant were measured by ELISA. (C) BSA (100 μg/ml; Control), AGE2 (100 μg/ml), and *P*-LPS (250 ng/ml) pre-treated osteocytes and osteoblastic cells were co-cultured in medium with (closed column) or without (open column) the sclerostin-neutralizing antibody (2 μg/ml) for 24 h. ALPase activity in osteoblastic cells was assessed according to the methods described in the Materials and methods section. (D) Total RNA was isolated from co-cultured osteoblastic cells, and Runx2 mRNA was analyzed by a quantitative RT-PCR. Runx2 mRNA expression was normalized by GAPDH mRNA expression. Data of protein and RNA samples are expressed as the means ± SD of four and six cultures, respectively. Asterisks show a significant difference (*$P < 0.05$, **$P < 0.01$).

mouse pre-osteoblastic cells were cultured with sclerostin, ALPase activity was slightly inhibited and calcium deposition was clearly suppressed [60]. In the present co-culture system with MLO-Y4-A2 cells (osteocyte) and MC3T3-E1 cells (osteoblastic cells), ALPase activity and Runx2 expression in osteoblastic cells that were co-cultured with osteocytes treated by AGEs and *P*-LPS was significantly decreased, and the sclerostin-neutralizing antibody restored ALPase activity and Runx2 expression. ALPase and Runx2 are important factor in osteoblastic differentiation, and these expressions are regulated by Wnt/β-catenin signaling [61]. Vega et al. reported that when β-catenin was knocked down using siRNA, Runx2 protein production was significantly decreased [62].

Although the effects of AGEs and *P*-LPS on BMP signaling and calcification in osteoblastic cells via the sclerostin pathway currently remain unknown, AGEs and *P*-LPS inhibited the differentiation of osteoblastic cells by up-regulating sclerostin expression. Therefore, AGEs and *P*-LPS exert catabolic effects on the metabolism of alveolar bone and inflammation, and may aggravate periodontitis with DM.

Supplementary data to this article can be found online at https://doi.org/10.1016/j.bone.2019.02.001.

Acknowledgments

This study was supported by a Grant-in-Aid for Young Scientist (B) (No. 16K20674) from the Japan Society for the Promotion of Science. IDG-SW3 cells were kindly supplied by Dr. Masahiro Hiasa (Department of Orthodontics, Institute of Biomedical Sciences, Tokushima University Graduate School).

References

[1] H. Chen, T. Senda, K.Y. Kubo, The osteocyte plays multiple roles in bone remodeling and mineral homeostasis, Med. Mol. Morphol. 48 (2) (2015) 61–68.
[2] G.Y. Rochefort, S. Pallu, C.L. Benhamou, Osteocyte: the unrecognized side of bone tissue, Osteoporos. Int. 21 (9) (2010) 1457–1469.
[3] S. Bhattacharyya, S. Pal, N. Chattopadhyan, Targeted inhibition of sclerostin for post-menopausal osteoporosis therapy: a critical assessment of the mechanism of action, Eur. J. Pharmacol. 826 (2018) 39–47.
[4] M. Sharifi, L. Ereifej, E.M. Lewiecki, Sclerostin and skeletal health, Rev. Endocr. Metab. Disord. 16 (2) (2015) 149–156.
[5] A.R. Wijenayaka, M. Kogawa, H.P. Lim, L.F. Bonewald, D.M. Findlay, G.J. Atkins, Sclerostin stimulates osteocyte support of osteoclast activity by a RANKL-dependent pathway, PLoS One 6 (10) (2011) e25900.
[6] G.G. Loots, M. Kneissel, H. Keller, M. Baptist, J. Chang, N.M. Collette, D. Ovcharenko, I. Plajzer- Frick, E.M. Rubin, Genomic deletion of a long-range bone enhancer misregulates sclerostin in Van Buchem disease, Genome Res. 15 (7) (2005) 928–935.
[7] F. Cosman, D.B. Crittenden, J.D. Adachi, N. Binkley, E. Czerwinski, S. Ferrari, L.C. Hofbauer, E. Lau, E.M. Lewiecki, A. Miyauchi, C.A. Zerbini, C.E. Milmont, L. Chen, J. Maddox, P.D. Meisner, C. Libanati, A. Grauer, Romosozumab treatment in postmenopausal woman with osteoporosis, N. Engl. J. Med. 375 (16) (2016) 1532–1543.
[8] J.T. Compton, F.Y. Lee, A review of osteocyte function and the emerging importance of sclerostin, J. Bone Joint Surg. Am. 96 (19) (2014) 1659–1668.
[9] A. Garcia-Martin, P. Rozas-Moreno, R. Reyes-Garcia, S. Morales-Santana, B. Garcia-Fontana, J.A. Garcia-Salcedo, M. Muñoz-Torres, Circulating levels of sclerostin are increased in patients with type 2 diabetes mellitus, J. Clin. Endocrinol. Metab. 97 (1) (2012) 234–241.
[10] M.F. Faienza, A. Ventura, M. Delvecchio, A. Fusillo, L. Piacente, G. Aceto, G. Colaianni, S. Colucci, L. Cavallo, M. Grano, G. Brunetti, High sclerostin and dickkop-1 (Dkk1) serum levels in children adolescents with type 1 diabetes mellitus, J. Clin. Endocrinol. Metab. 102 (4) (2017) 1174–1181.
[11] M. Yamamoto, M. Yamauchi, T. Sugimoto, Elevated sclerostin levels are associated with vertebral fractures in patients with type 2 diabetes mellitus, J. Clin. Endocrinol. Metab. 98 (10) (2013) 4030–4037.
[12] A. Di Benedetto, I. Gigante, S. Colucci, M. Grano, Periodontal disease: linking the primary inflammation to bone loss, Clin. Dev. Immunol. 2013 (2013) 503754.
[13] R.S. Gomez, W.O. Dutra, P.R. Moreira, Epigenetics and periodontal disease: future perspectives, Inflamm. Res. 58 (10) (2009) 625–629.
[14] M. Suzuki, M. Yoneda, T. Hirofuji, Mixed red-complex bacterial infection in periodontitis, Int. J. Dent. Clin. 2103 (2013) 587279.
[15] S. Jain, R.P. Darveau, Contribution of *Porphyromonas gingivalis* lipopolysaccharide to periodontitis, Periodontol. 2000 54 (1) (2010) 53–70.
[16] H. Kadono, J. Kido, M. Kataoka, N. Yamauchi, T. Nagata, Inhibition of osteoblastic cell differentiation by lipopolysaccharide extract from *Porphyromonas gingivalis*, Infect. Immun. 67 (6) (1999) 2841–2846.
[17] H.C. Roberts, R. Moseley, A.J. Sloan, S.J. Youde, R.J. Waddington, Lipopolysaccharide alters decorin and biglycan synthesis in rat alveolar bone osteoblasts: consequences for bone repair during periodontal disease, Eur. J. Oral Sci. 116 (3) (2008) 207–216.
[18] N. Bostanci, G.N. Belibasakis, *Porphyromonas gingivalis*: an invasive and evasive opportunistic oral pathogen, FEMS Microbiol. Lett. 333 (1) (2012) 1–9.
[19] B.L. Pihlstrom, B.S. Michalowicz, N.W. Johnson, Periodontal disease, Lancet 366 (9499) (2005) 1809–1820.
[20] H. Löe, Periodontal disease. The sixth complication of diabetes mellitus, Diabetes Care 16 (1) (1993) 329–334.
[21] B.L. Mealey, G.L. Ocampo, Diabetes mellitus and periodontal disease, Periodontol.

2000 44 (2007) 127–153.
[22] S.Y. Goh, M.E. Cooper, Clinical review, The role of advanced glycation end products in progression and complications of diabetes, J. Clin. Endocrinol. Metab. 93 (4) (2008) 1143–1152.
[23] Y. Morioka, K. Teshigawara, Y. Tomono, D. Wang, Y. Izushi, H. Wake, K. Liu, H.K. Takahashi, S. Mori, M. Nishibori, The specific localization of advanced glycation end-products (AGEs) in rat pancreatic islets, J. Pharmacol. Sci. 134 (4) (2017) 218–224.
[24] C.P. Sanches, A.G.D. Vianna, F.C. Barreto, The impact of type 2 diabetes on bone metabolism, Diabetol. Metab. Syndr. 9 (2017) 85.
[25] M. Yamamoto, T. Sugimoto, Advanced glycation end products, diabetes, and bone strength, Curr. Osteoporos. Rep. 14 (6) (2016) 320–326.
[26] A. Zizzi, G. Tirabassi, S.D. Aspriello, M. Piemontese, C. Rubini, G. Lucarini, Gingival advanced glycation end-products in diabetes mellitus-associated chronic periodontitis: an immunohistochemical study, J. Periodontal Res. 48 (3) (2013) 293–301.
[27] S.K. Sonneschein, J. Meyie, Local inflammatory reactions in patients with diabetes and periodontitis, Periodontol. 2000 69 (1) (2015) 221–254.
[28] N. Ogawa, T. Yamaguchi, S. Yano, M. Yamauchi, M. Yamamoto, T. Sugimoto, The combination of high glucose and advanced glycation end-products (AGEs) inhibits the mineralization of osteoblastic MC3T3-E1 cells through glucose-induced increase in the receptor for AGEs, Horm. Metab. Res. 39 (12) (2007) 871–875.
[29] E. Sakamoto, C. Mihara, T. Ikuta, Y. Inagaki, J. Kido, T. Nagata, Inhibitory effects of advanced glycation end-products and *Porphyromonas gingivalis* lipopolysaccharide on the expression of osteoblastic markers of rat bone marrow cells in culture, J. Periodontal Res. 51 (3) (2016) 312–320.
[30] M.H. Napimoga, C. Nametala, F.L. da Silva, T.S. Miranda, J.P. Bossonaro, A.P. Demasi, P.M. Duarte, Involvement of the Wnt-β-catenin signalling antagonists, sclerostin and dickkopf-related protein 1, in chronic periodontitis, J. Clin. Periodontol. 41 (6) (2014) 550–557.
[31] U. Balli, A. Aydogdu, F.O. Dede, C.C. Turer, B. Guven, Gingival crevicular fluid levels of sclerostin, osteoprotegerin, and receptor activator of nuclear factor-κB ligand in periodontitis, J. Periodontol. 86 (12) (2015) 1396–1404.
[32] K. Okazaki, T. Yamaguchi, K. Tanaka, M. Notsu, N. Ogawa, S. Yano, T. Sugimoto, Advanced glycation end products (AGEs), but not high glucose, inhibit the osteoblastic differentiation of mouse stromal ST2 cells through the suppression of osterix expression, and inhibit cell growth and increasing cell apoptosis, Calcif. Tissue Int. 91 (4) (2012) 286–296.
[33] O.H. Lowry, N.R. Roberts, M.L. Wu, E.J. Crawford, The quantitative histochemistry of brain. II Enzyme measurements, J. Biol. Chem. 207 (1) (1954) 19–37.
[34] F. Nishimura, T. Kono, C. Fujimoto, Y. Iwamoto, Y. Murayama, Negative effects of chronic inflammatory periodontal disease on diabetes mellitus, J. Int. Acad. Periodontol. 2 (2) (2000) 49–55.
[35] T. Saito, Y. Shimazaki, Y. Kiyohara, I. Kato, M. Kubo, M. Iida, T. Koga, The severity of periodontal disease is associated with the development of glucose intolerance in non-diabetics: the Hisayama study, J. Dent. Res. 83 (6) (2004) 485–490.
[36] Y.S. Khader, A.S. Dauod, S.S. El-Qaderi, A. Alkafajei, W.Q. Batayha, Periodontal status of diabetics compared with nondiabetics: a meta-analysis, J. Diabetes Complicat. 20 (1) (2006) 59–68.
[37] L. Ren, Y. Fu, Y. Deng, L. Qi, L. Jin, Advanced glycation end products inhibit the expression of collagen type I and III by human gingival fibroblasts, J. Periodontol. 80 (7) (2009) 1166–1173.
[38] S. Yu, H. Li, Y. Ma, Y. Fu, Matrix metalloproteinase-1 of gingival fibroblasts influenced by advanced glycation end products (AGEs) and their association with receptor for AGEs and nuclear factor-κB in gingival connective tissue, J. Periodontol. 83 (1) (2012) 119–126.
[39] K. Tanaka, T. Yamaguchi, I. Kanazawa, T. Sugimoto, Effects of high glucose and advanced glycation end products on the expressions of sclerostin and RANKL as well as apoptosis in osteocyte-like MLO-Y4-A2 cells, Biochem. Biophys. Res. Commun. 461 (2) (2015) 193–199.
[40] M. Notsu, I. Kanazawa, A. Takeno, M. Yokomoto-Umakoshi, K.I. Tanaka, T. Yamaguchi, T. Sugimoto, Advanced glycation end product 3 (AGE3) increase apoptosis and the expression of sclerostin by stimulating TGF-β expression and secretion in osteocyte-like MLO-Y4-A2 cells, Calcif. Tissue Int. 100 (4) (2017) 402–411.
[41] J.H. Kim, D.E. Lee, G.H. Woo, J.H. Cha, E.J. Bak, Y.J. Yoo, Osteocytic sclerostin expression in alveolar bone in rats with diabetes mellitus and ligature-induced periodontitis, J. Periodontol. 86 (8) (2015) 1005–1011.
[42] H. Chen, W. Liu, X. Wu, M. Gou, J. Shen, H. Wang, Advanced glycation end products induced IL-6 and VEGF-A production and apoptosis in osteocyte-like MLO-Y4 cells by activating RAGE and ERK1/2, P38 and STAT3 signaling pathways, Int. Immunopharmacol. 52 (2017) 143–149.
[43] K. Nonaka, Y. Kajiura, M. Bando, E. Sakamoto, Y. Inagaki, J.H. Lew, K. Naruishi, T. Ikuta, K. Yoshida, T. Kobayashi, H. Yoshie, T. Nagata, J. Kido, Advanced glycation end-products increase IL-6 and ICAM-1 expression via RAGE, MAPK and NF-κB pathways in human gingival fibroblasts, J. Periodontal Res. 53 (3) (2018) 334–344.
[44] H. Kato, Y. Taguchi, K. Tominaga, M. Umeda, A. Tanaka, *Porphyromonas gingivalis* LPS inhibits osteoblastic differentiation and promotes pro-inflammatory cytokine production in human periodontal ligament stem cells, Arch. Oral Biol. 59 (2) (2014) 167–175.
[45] J.H. Ross, D.C. Hardy, C.A. Schuyler, E.H. Slate, T.W. Mize, Y. Huang, Expression of periodontal interleukin-6 protein is increased across patients with neither periodontal disease nor diabetes, patients with periodontal disease alone and patients with both disease, J. Periodontal Res. 45 (5) (2010) 688–694.
[46] Y. Yamamoto, A. Harashima, H. Saito, K. Tsuneyama, S. Munesue, S. Motoyoshi, D. Han, T. Watanabe, M. Asano, S. Takasawa, H. Okamoto, S. Shimura, T. Karasawa, H. Yonekura, H. Yamamoto, Septic shock is associated with receptor for advanced glycation end products ligation of LPS, J. Immunol. 186 (5) (2011) 3248–3257.
[47] A. Pollreisz, B.I. Hudson, J.S. Chang, W. Qu, B. Cheng, P.N. Papapanou, A.M. Schmidt, E. Lalla, Receptor for advanced glycation endproducts mediates pro-atherogenic responses to periodontal infection in vascular endothelial cells, Atherosclerosis 212 (2) (2010) 451–456.
[48] A. Kassem, P. Henning, P. Lundberg, P.P. Souza, C. Lindholm, U.H. Lerner, *Porphyromonas gingivalis* stimulates bone resorption by enhancing RANKL (Receptor Activator of NF-κB Ligand) through activation of toll-like receptor 2 in osteoblasts, J. Biol. Chem. 290 (33) (2015) 20147–20158.
[49] P. Zhang, J. Liu, Q. Xu, G. Harber, X. Feng, S.M. Michalek, J. Katz, TLR2-dependent modulation of osteoclastogenesis by *Porphyromonas gingivalis* through differential induction of NFATc1 and NF-kappa B, J. Biol. Chem. 286 (27) (2011) 24159–24169.
[50] J. Lei, Z. Wang, D. Hui, W. Yu, D. Zhou, W. Xia, C. Chen, Q. Zhang, Z. Wang, Q. Zhang, A.P. Xiang, Ligation of TLR2 and TLR4 on murine bone marrow-derived mesenchymal stem cells triggers differential effects on their immunosuppressive activity, Cell. Immunol. 271 (1) (2011) 147–156.
[51] C. Vincent, D.M. Findlay, K.J. Welldon, A.R. Wijenayaka, T.S. Zheng, D.R. Haynes, N.L. Fazzalari, A. Evdokiou, G.J. Atkins, Pro-inflammatory cytokines TNF-related weak inducer of apoptosis (TWEAK) and TNF alpha induce the mitogen-activated protein kinase (MAPK)-dependent expression of sclerostin in human osteoblasts, J. Bone Miner. Res. 24 (8) (2009) 1434–1449.
[52] H.Z. Meng, W.L. Zhang, F. Liu, M.W. Yang, Advanced glycation end products affect osteoblast proliferation and function by modulating autophagy via the receptor of advanced glycation end products/Raf protein/mitogen-activated protein kinase/extracellular signal-regulated kinase kinase/extracellular signal-regulated kinase (RAGE/Raf/MEK/ERK) pathway, J. Biol. Chem. 290 (47) (2015) 28189–28199.
[53] S. Franke, C. Röster, J. Pester, G. Hofmann, P. Oelazner, G. Wolf, Advanced glycation end products affect growth and function of osteoblasts, Clin. Exp. Rheumatol. 29 (4) (2011) 650–660.
[54] J.J. Westendorf, R.A. Kahler, T.M. Schroeder, Wnt signaling in osteoblasts and bone disease, Gene 341 (2004) 19–39.
[55] Y. Han, X. You, W. Xing, Z. Zhang, W. Zou, Paracrine and endocrine actions of bone-the functions of secretory proteins from osteoblasts, osteocytes and osteoclasts, Bone Res. 6 (2018) 16.
[56] P. Duan, L.F. Bonewald, The role of the Wnt/β-catenin signaling pathway in formation and maintenance of bone and teeth, Int. J. Biochem. Cell Biol. 77 (Pt A) (2016) 23–29.
[57] C. Hamann, M. Rauner, Y. Höhna, R. Bernhardt, J. Mettelsiefen, C. Goettsch, K.P. Günther, M. Stolina, C.Y. Han, F.J. Asuncion, M.S. Ominsky, L.C. Hofbauer, Sclerostin antibody treatment improves bone mass, bone strength, and bone defect regeneration in rats with type 2 diabetes mellitus, J. Bone Miner. Res. 28 (3) (2013) 627–638.
[58] D.G. Winkler, M.K. Sutherland, J.C. Geoghegan, C. Yu, T. Hayes, J.E. Skonier, D. Shpektor, M. Jonas, B.R. Kovacevich, K. Staehling-Hampton, M. Appleby, M.E. Brunkow, J.A. Latham, Osteocyte control of bone formation via sclerostin, a novel BMP antagonist, EMBO J. 22 (23) (2003) 6267–6276.
[59] S. Liu, A.S. Virdi, K. Sena, D.R. Sumner, Sclerostin antibody prevents particle-induced implant loosening by stimulating bone formation and inhibiting bone resorption in a rat model, Arthritis Rheum. 64 (12) (2012) 4012–4020.
[60] R.L. van Bezooijen, B.A. Roelen, A. Visser, L. van der Wee-Pals, E. de Wilt, M. Karperien, H. Hamersma, S.E. Papapoulos, P. ten Dijke, C.W. Löwik, Sclerostin is an osteocyte-expressed negative regulator of bone formation, but not a classical BMP antagonist, J. Exp. Med. 199 (6) (2004) 805–814.
[61] Y. Kobayashi, S. Uehara, N. Udagawa, N. Takahashi, Regulation of bone metabolism by Wnt signals, J. Biochem. 159 (4) (2016) 287–292.
[62] O.A. Vega, C.M.J. Lucero, H.F. Araya, S. Jerez, J.C. Tapia, M. Antonelli, F. Salazar-Onfray, F. Las Heras, R. Thaler, S.M. Riester, G.S. Stein, A.J. van Wijnen, M.A. Galindo, Wnt/b-catenin signaling activates expression of the bone-related transcription factor RUNX2 in select human osteocarcome cell types, J. Cell. Biochem. 118 (11) (2017) 3662–3674.